

Dynamics of the Contacts reveals Widom Lines for Jamming

C. COULAIS¹, R. P. BEHRINGER² and O. DAUCHOT³

¹ *SPHYNX/SPEC, CEA-Saclay, URA 2464 CNRS, 91 191 Gif-sur-Yvette, France*

² *Department of Physics and Center for Nonlinear and Complex Systems, Duke University, Durham, North Carolina 27708-0305, USA*

³ *EC2M, ESPCI-ParisTech, UMR Gulliver 7083 CNRS, 75005 Paris, France*

PACS 45.70.Vn – Granular models of complex systems.

PACS 45.70.Cc – Compaction, granular systems.

PACS 64.60.Ht – Critical points, dynamic critical behavior.

Abstract – We experimentally study the vicinity of the Jamming transition by investigating the statics and the dynamics of the contact network of a horizontally shaken bi-disperse packing of photo-elastic discs. Compressing the packing very slowly, while maintaining a mechanical excitation, yields a granular glass, namely a frozen structure of vibrating grains. In this glass phase, we observe a remarkable dynamics of the *contact network*, which exhibits strong dynamical heterogeneities. Such heterogeneities are maximum at a packing fraction ϕ^* , *distinct* and smaller than the structural packing fraction ϕ^\dagger , which is indicated by an abrupt variation of the average number of contact per particle. We demonstrate that the two cross-overs, one for the maximum dynamical heterogeneity, and the other for static jamming, converge at point J in the zero mechanical excitation limit, a behavior reminiscent of the Widom lines in the supercritical phase of a second order critical point. Our findings are discussed in the light of recent numerical and theoretical studies of thermal soft spheres.

At large packing fraction, disordered packings of particles with repulsive contact interactions jam into a rigid state. For frictionless and a-thermal particles, the jamming transition coincides with the onset of isostaticity and a number of geometrical and mechanical quantities exhibit clear scaling laws with the distance to jamming [1]. One prominent signature of jamming is the singular behavior of the average number of contacts per particle $z - z_J \propto (\phi - \phi_J)^{0.5}$, where $z_J = 2d$, d being the space dimension [2,3]. The distribution of the gaps between particles displays a delta function at zero and a square root decay for increasing gaps, which is key to the singular behavior of the average contact number [4–7].

Although the average coordination number singularity is the hallmark of jamming at zero temperature, its behavior is less clear at finite temperature. Both experimentally [8] and numerically, [6,8–11] it has been observed that the first peak of the partial pair correlation function has a finite maximum at a packing fraction $\phi_j(T) > \phi_j(0) = \phi_J$. This maximum has been interpreted as a vestige of the divergence of the pair correlation function at point J, the $T = 0$ jamming transition. (fig. 1). However, it was later argued [12], that this structural anomaly can be accounted

for using equilibrium liquid state theory, and is therefore not specific to Jamming. The vicinity of point J has also been explored in a mean-field-like replica description of thermal soft and hard spheres [13]. This description recovers all the observed scalings in temperature and packing fraction *but* the square root singularity of the pair correlation function when $T = 0^+$ and $\phi = \phi_J^+$. This discrepancy, together with the onset of a diverging length in the vibrational properties of the jammed state [14], suggest that larger scale correlations must be taken into account, and calls for a better characterization of the vicinity of point J.

In the present letter, we focus on the *dynamics* of the contact network, a natural quantity of interest as soon as dynamics is present, which, to our knowledge, has never been explored so far. To this end, we experimentally investigate a vibrated two-dimensional bi-disperse packing of photo-elastic grains, close to its jamming transition. We control both the packing fraction, ϕ , and the mechanical excitation, γ , to be defined precisely below. This mechanically driven and dissipative system is far from equilibrium and the mechanical excitation is different from a temperature in many aspects. However, by analogy, one can rea-

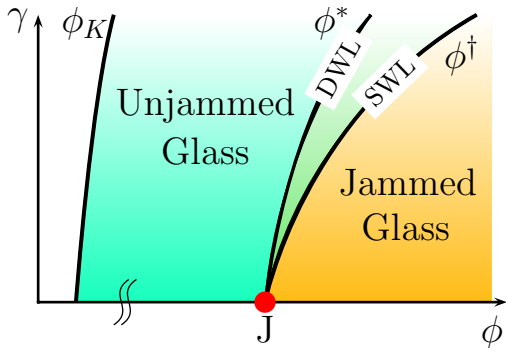


Fig. 1: **Sketch of phase space.** (color online) In the glass phase, two Widom lines, a structural one (SWL) and a dynamical one (DWL) emerge from point J and separate the jammed glass (frozen structure and frozen contacts) from the unjammed one (frozen structure but "liquid" contacts).

sonably consider that both temperature and mechanical excitation provide agitation to the particles. The structure, in terms of particle neighborhoods, is completely frozen on the experimental time scales: the system can safely be considered as a granular glass. The structural signature of jamming $\phi^\dagger(\gamma)$ is given by an abrupt variation of the average number of contacts. Above $\phi^\dagger(\gamma)$, the contacts are also frozen. On the contrary below $\phi^\dagger(\gamma)$, they exhibit a rich dynamics with strong heterogeneities. For any finite mechanical excitation γ , these heterogeneities are maximum at a packing fraction $\phi^*(\gamma)$ smaller than $\phi^\dagger(\gamma)$. The relative shift $|\epsilon^*| = |\phi^* - \phi^\dagger|/\phi^\dagger$ decreases linearly towards zero and the characteristic length of the dynamical heterogeneities eventually diverges as the mechanical excitation approaches zero. Our results suggest the phase space diagram sketched in Fig. 1, where the structural and the dynamical crossovers are reminiscent of Widom lines [15, 16] for point J, namely the locus of the maxima of the second derivatives of the free energy, introduced in the context of critical phenomena.

Our experimental set up (Fig. 2 a) is adapted from [17, 18], and allows us to shake photoelastic discs between two cross-polarizers, thereby accessing the contact and force network [3, 19]. A bi-disperse mixture of 4964 and 3216 polyurethane (PSM-4) discs, of respectively 4mm and 5mm diameter, lies on a flat transparent surface, which oscillates with an amplitude of 1 cm at different frequencies of 6.25, 7.5 or 10 Hz. For frequencies smaller than $f_0 = 4.17$ Hz, the grains do not slip on the plate and the mechanical excitation is effectively null. In the following we shall use the reduced frequency $\gamma = (f - f_0)/f_0$ as a measure of the mechanical excitation. The grains are confined in a static rectangular cell, for which the position of one horizontal boundary is tuned using a micro-metric piston attached to a force sensor. A LED back-light and a circular polarizing sheet are inserted in the vibrating surface, so that the grains are lighted by transmission of circularly polarized light. A monochromatic high resolu-

tion CCD camera records two types of images in phase with the vibration. Every odd period, a circular analyzer is inserted by a rotating wheel in the camera field to visualize the photoelastic pattern. From the direct-light images acquired every even period, we obtain the grain positions with a resolution of 0.5% of the mean grain diameter. We then use standard tracking and tessellation techniques to obtain the dynamics and structure of the packings. From the cross-polarized images, we estimate the normal force between two neighbors by integrating the square spatial gradient of the light intensity over the area defined by the two Delaunay triangles sharing a common edge. Henceforth, all lengths are expressed in units of the small grain diameter, and time is expressed in units of vibration cycles.

In order to ensure the highest and most reproducible jammed packings, the packing fraction, which we control with a relative resolution of 5×10^{-6} is increased by steps of $\delta\phi = 3 \times 10^{-4}$ to some maximum value, using exponentially increasing time steps (Fig. 3 b). All images are then acquired during stepwise decompression. For each decompression step we carefully check that the system reaches a steady state, and all data presented here have been computed in this steady regime. Fig. 3 (c) displays the pressure with respect to the packing fraction. P_{TOT} (respectively P_{STAT}) is the pressure measured when the vibration is switched on (respectively off). P_{STAT} is thus the static pressure sustained by the packing in the absence

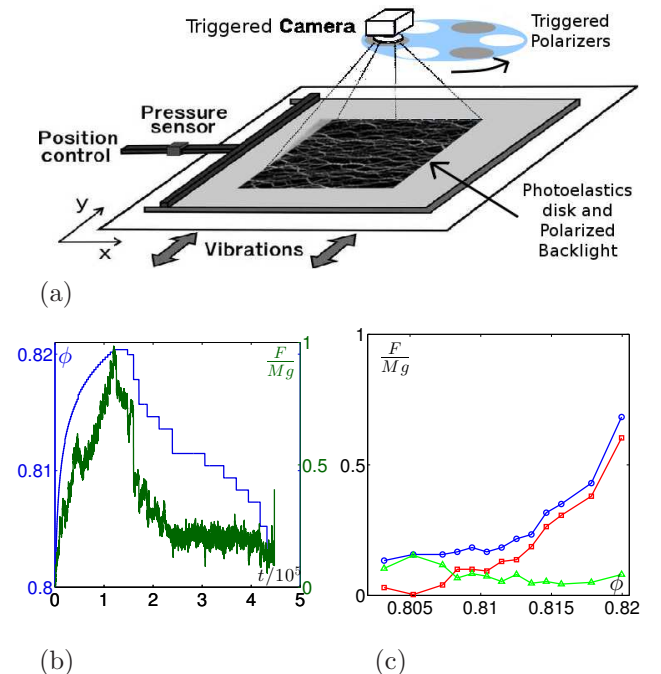


Fig. 2: **Experimental setup and protocol.** (color online) (a): The vibrating cell. (b): Logarithmic increase followed by a stepwise decrease of the packing fraction, and pressure at the wall. (c): Average pressure vs packing fraction, $\gamma = 1.4$: (○) : P_{TOT} , (□) : P_{STAT} , (△) : P_{DYN} as defined in the text.

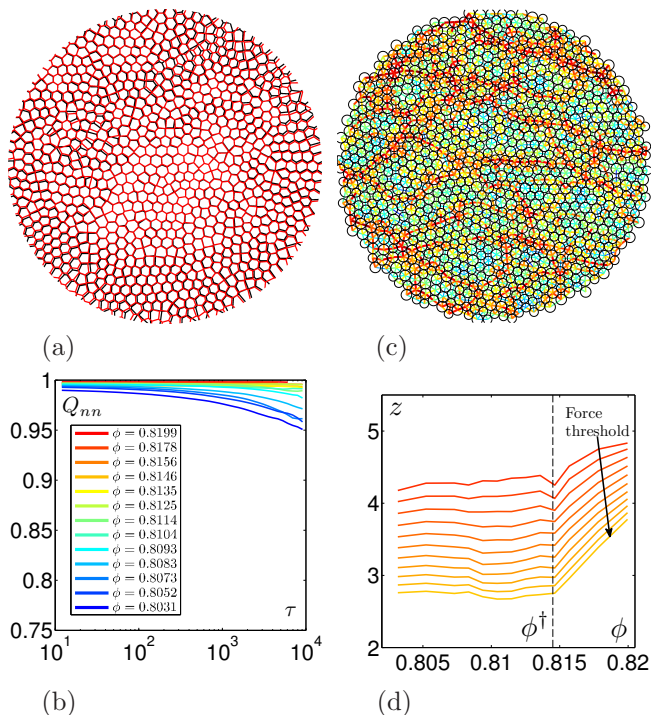


Fig. 3: **Structure of the granular glass**, $\gamma = 1.4$ (color online) (a): Superposition of the Laguerre cells computed at times $t = 1$ and $t = 5000$ for the loosest packing ($\phi = 0.8031$). (b): Average fraction of neighbors $Q_{nn}(\tau)$ which have not changed between two images separated by a time interval τ , for different packing fractions, as indicated in the legend. (c): map of contact forces. Red colors stand for high forces and bluer color stand for low forces. (d): Average coordination number z vs. packing fraction ϕ , determined according to various force thresholds

of vibration, whereas $P_{DYN} = P_{TOT} - P_{STAT}$ can be interpreted as the additional dynamic pressure, induced by the vibration. At high packing fraction, the pressure is dominated by its static part, whereas at low packing fraction, it is mostly dynamic. A crossover occurs at some intermediate packing fraction, which in [17] was shown to coincide with a maximum in the heterogeneity of the dynamics, as probed at scales of the order of 10^{-2} grain diameter. Here, the transition is shifted to lower values of ϕ , a fact which we attribute to the higher interparticle friction of the photoelastic discs [1]. Also the transitional range is wider, which is likely due to the relative softness of the photoelastic discs as compared to the brass discs used in earlier experiments. (Young modulus of 0.5GPa, as compared to 100GPa).

We first focus on the largest mechanical excitation level, $\gamma = 1.4$. Altogether, the above compression protocol produces a structure in terms of nearest neighbor relationships, which is completely frozen on experimental timescales. The Laguerre tessellation of two different packings separated by a time lag 5000 can be superimposed almost perfectly, even at the loosest packing fraction (Fig. 3 (a)). This is further quantified by $Q_{nn}(\tau)$, the

average fraction of *neighbor* relationships surviving in a time interval τ . Q_{nn} remains larger than 95% even for the loosest packing fraction, and is barely less than 100% for the denser ones (Fig. 3(b)). The contact network within this frozen structure is provided by an analysis of the photoelastic images. A threshold is applied to both the gap between neighboring particles and the contact force (see map of contact forces in fig. 3 (c)), to decide what particles are in contact. Fig. 3 (d) displays the average number of contacts, z , as a function of the packing fraction for different thresholds. While the absolute value of z depends on the threshold, the dependence on ϕ is very robust: z is constant at low packing fractions, displays a kink at some intermediate packing fraction, and thereafter, increases. The kink occurs at a packing fraction which is independent of the threshold. We interpret this packing fraction as the signature of a structural crossover to jamming in the presence of vibration and find $\phi^\dagger = 0.8143 \pm 0.0005$. Above ϕ^\dagger , the system is jammed and, $z \sim a(\phi - \phi^\dagger)^\beta + z_c$, where $\beta \in [0.4, 1]$ and $z_c \in [2.7, 4.3]$ depend on the threshold. Since counting arguments for frictional packings [1] constrain z_c between 3 and 4 for two-dimensional systems, it is fair to say that the transition indicated by the kink is robust to the thresholding procedure. We now come to the innovative part of this work, which consists of studying the *dynamics* of the contact network and its dependence on the mechanical excitation.

Analyzing the force network, we recover existing results on the force distributions [20] and observe that its dynamics is slaved to that of the contacts. We thus concentrate on the description of the dynamics of the contact network. It is naturally quantified by an estimator of the contact overlap between t and $t + \tau$:

$$Q^z(t, \tau) = \frac{1}{N} \sum_i Q_i^z(t, \tau), \quad (1)$$

where $Q_i^z(t, \tau) = \Theta(2 - |\delta z_i(t, \tau)|)$, with $\Theta(\cdot)$, the Heavy-side function and $\delta z_i(t, \tau)$, the change in number of contact of grain i , between t and $t + \tau$. Alternative definitions, e.g. requiring smaller or larger local contact fluctuations, do not change the following conclusions. Fig. 4 (a) displays $Q_z(\tau) = \langle Q^z(t, \tau) \rangle_t$ for the various packing fractions, where $\langle \cdot \rangle_t$ denotes the time average. The black curve corresponds to the packing fraction of the jamming crossover ϕ^\dagger . For $\phi > \phi^\dagger$, $Q^z(\tau)$ remains constant at values ranging between 0.7 and 0.9, indicating that there is no long-time decorrelation of the contact network: the contacts are established permanently, once they are formed. The sole decorrelation observed above ϕ^\dagger occurs at short times and is induced by the fast dynamics of the rattlers, the number of which increases when ϕ approaches ϕ^\dagger . For $\phi < \phi^\dagger$, long time relaxation clearly sets in, indicating that contacts now rearrange. One can thus think about this structural crossover as a glass transition for the binary degrees of freedom (e.g. yes/no) which indicate whether neighboring particles are in contact or not. Accordingly, one would

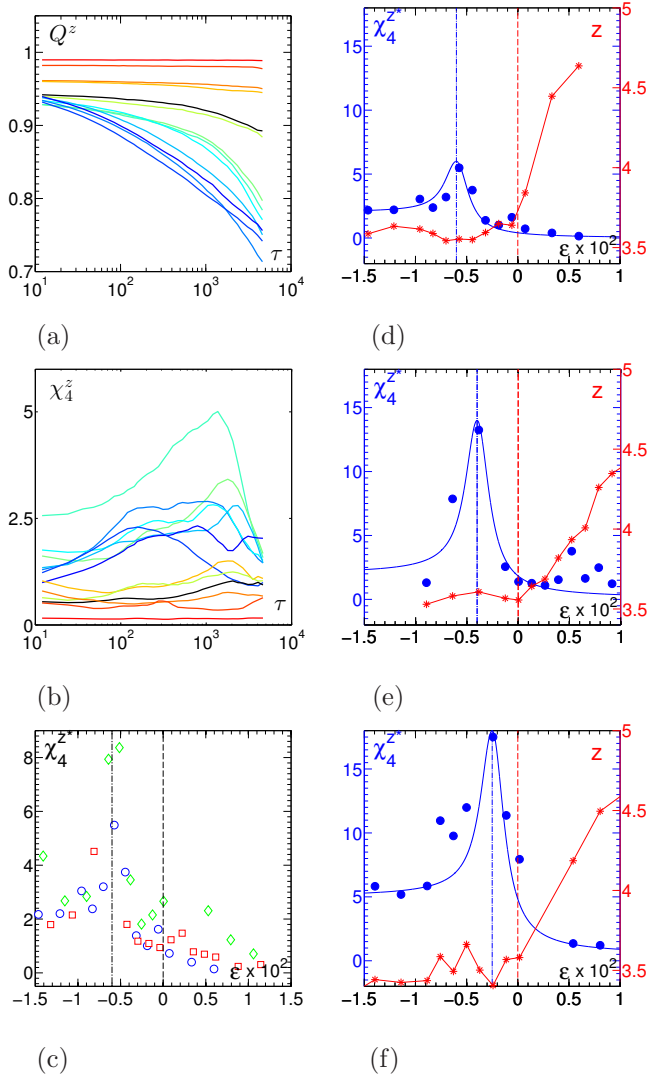


Fig. 4: **Contact Dynamics** (color online). **(a)**: Average contact overlap $Q_z^z(\tau)$ for different packing fractions, $\gamma = 1.4$ (same color code as in fig. 3 (a) with the curve corresponding to ϕ_J plotted in black). **(b)**: Contact overlap dynamical susceptibility $\chi_4^z(\tau)$, $\gamma = 1.4$ (same color code). **(c)**: Contact overlap dynamical susceptibility χ_4^{z*} , chosen for the delay time, τ , that maximizes its value, as a function of $\epsilon = (\phi^* - \phi^\dagger)/\phi^\dagger$ for three realizations (\bullet , \square , \diamond) of the same experiment, $\gamma = 1.4$. **(d,e,f)**: Maximal contact overlap dynamical susceptibility χ_4^{z*} (\bullet) and average contact number z (\star) versus ϵ for three different amplitudes of the vibration: (d) $\gamma = 1.4$; (e) $\gamma = 0.8$; (f) $\gamma = 0.5$. The red, respectively blue, dashed line indicates the location of ϕ^* , resp. ϕ^\dagger . The continuous blue curve is a guide to the eye.

like to further investigate this long term dynamics, in order to see whether it shares other similarities with glassy dynamics in spin systems.

We compute the dynamical susceptibility (see [21] for an introduction to dynamical heterogeneities):

$$\chi_4^z(\tau) = N \frac{\text{Var}(Q^z(t, \tau))}{\langle \text{Var}(Q_i^z(t, \tau)) \rangle_i}, \quad (2)$$

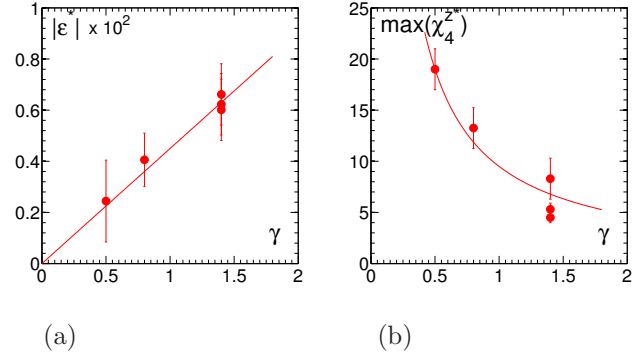


Fig. 5: **Dependence on the vibration amplitude** (color online) of **(a)** $|\epsilon^*|$, the relative shift between ϕ^* and ϕ^\dagger and **(b)** the maximal dynamical susceptibility as a function of the vibration amplitude γ . The continuous lines indicate, respectively, a linear and a $1/\gamma$ dependence on γ .

where $\text{Var}(\cdot)$ denotes the variances sampled over time and $\langle \cdot \rangle_i$ denotes the average over the grains. This dynamic susceptibility estimates the range of the spatial correlation in the dynamics of the contact network. One sees in Fig. 4 (b) that $\chi_4^z(\tau)$ becomes significant for $\phi < \phi^\dagger$ and then exhibits a maximum χ_4^{z*} in time, which in turn displays a clear maximum at a packing fraction ϕ^* . Performing three independent experimental runs, with the same vibration $\gamma = 1.4$, we observe in fig. 4(c) that ϕ^* is systematically smaller than ϕ^\dagger , with a relative shift $\epsilon^* = (\phi^* - \phi^\dagger)/\phi^\dagger = -5 \times 10^{-3}$: the reorganization of the contacts is maximally collective, indicating a dynamical crossover *below* ϕ^\dagger . Since it is well known that the jamming transition and its related crossovers, a priori depend on the initial conditions and the preparation protocol [22], we shall now use the reduced packing fraction $\epsilon = \phi - \phi^\dagger/\phi^\dagger$, in order to compare different experimental runs.

The robustness of our finding is further reinforced by the fact that we could demonstrate a systematic dependence on the excitation γ . Figures 4(d,e,f) display the dynamical susceptibility together with the average contact number as a function of the packing fraction for respectively $\gamma = 1.4, 0.8, 0.5$. On decreasing γ , one observes that (i) the dynamical crossover ϕ^* moves closer to the structural signature of jamming and (ii) the maximum of the dynamical susceptibility χ_4^{z*} , hence the correlation length, increases when γ decreases. Figure 5 summarizes these dependencies. Our data are compatible with a linear variation $|\epsilon^*| \propto \gamma$ and $\max(\chi_4^{z*}) \propto 1/\gamma$ suggesting a divergence of the correlation length at zero excitation.

Let us now summarize and discuss our observations. Having prepared a granular glass, with a frozen neighborhood structure, we have observed three salient features of the contact network: (i) the evolution of the averaged number of contacts with packing fraction, $z(\phi)$, points to a first transitional packing fraction ϕ^\dagger ; (ii) the dynamics of the contact network, together with the fluctuation of

the coordination number are maximally heterogeneous at a packing fraction $\phi^* < \phi^\dagger$. The shift in packing fraction decreases linearly with the amplitude of the mechanical excitation, while the dynamical heterogeneities increase sharply. This phenomenology, summarized in Fig. 1, is reminiscent of the so-called Widom lines observed in the supercritical region close to a critical point [15, 16]. To our knowledge, the present study is the first experimental characterization of these crossovers, including their dependence on the mechanical excitation. Obviously one would like to extend the range of dependence towards even lower excitation, but the required precision then calls for numerical investigations.

Along the way, our results address a long standing conundrum left from earlier experiments using the same apparatus, but with hard (brass) discs [17]. The authors observed a maximum in the heterogeneities of the dynamics for the packing fraction, where $P_{DYN}(\phi)$ and $P_{STAT}(\phi)$ intersect. The existence of this maximum suggests that the experiment probed both sides of the jamming transition, a puzzling conclusion given the very strong stiffness of the brass discs. Using soft discs, we demonstrate here that there are several signatures of point J at finite mechanical excitation, γ , and that the one associated with the dynamical heterogeneities occurs at a lower packing fraction, $\phi^*(\gamma)$, than the one at which the average number of contact increases, $\phi^\dagger(\gamma)$. The previous experiment using brass discs [17] was actually probing the dynamical crossover, ϕ^* , both sides of which lie below the structural signature of the jamming transition. This is further confirmed by the observation that, here also, $P_{DYN} \simeq P_{STAT}$ at ϕ^* .

Unlike thermal systems, our system is in an out-of-equilibrium, mechanically driven state. Still, recent numerical simulations [6, 9, 11, 23] suggest that for the kind of physics we are interested in, the similarities with thermal systems are much stronger than one may have expected at first sight. For instance, the structural crossover reported here might be related to the finite temperature first-peak pair-correlation maxima near the jamming point reported in [6, 8, 9]. More specifically, in [23] the authors report an extensive study of the dynamics close to point J, in the temperature-density space, which they conclude by comparing with existing colloidal experiments. To do so they essentially use the Debye-Waller factor, namely the size of the cage surrounding the particles, as a sensitive thermometer. In the present case, the cage size at the largest packing fraction and largest magnitude of excitation is of the order of 5×10^{-3} . This would correspond in Fig. 1 of their work to a rescaled kinetic energy of 10^{-6} . For lower excitation, it is even smaller. In all cases, we conclude that the present experiments, together with those of [17, 18] are for the moment the only ones, which have probed the dynamical criticality related to the jamming transition (see the discussion part and Fig. 12 in [23]). Whether the same scenario as the one described here holds for thermal soft spheres, such as emulsions, is an open issue for further

experimental investigation.

Finally, one cannot exclude the possible effect of friction. Here the friction coefficient amongst the grains is typically $\mu = 0.7$ and one indeed notes that the packing fractions of interest reported here have a lower value than those obtained for the brass discs ($\mu = 0.4$) and for frictionless particles. However our results demonstrate that at the qualitative level and in the dynamical regime probed by our set-up, friction does not seem to be a relevant parameter. Whether it impacts the quantitative scaling properties close to points J requires further studies, presumably numerical ones.

* * *

We acknowledge L. Berthier and F. Zamponi for illuminating discussions and are grateful to Cécile Wiertel-Gasquet and Vincent Padilla for their skillful technical assistance.

REFERENCES

- [1] VAN HECKE M., *Journal of Physics: Condensed Matter*, **22** (2010) 033101.
- [2] O'HERN C. S., LANGER S. A., LIU A. J. and NAGEL S. R., *Phys. Rev. Lett.*, **88** (2002) 075507.
- [3] MAJUMDAR T. S., SPERL M., LUDING S. and BEHRINGER R. P., *Phys. Rev. Lett.*, **98** (2007) 058001.
- [4] SILBERT L. E., ERTAŞ D., GREST G. S., HALSEY T. C. and LEVINE D., *Phys. Rev. E*, **65** (2002) 031304.
- [5] PARISI G. and ZAMPONI F., *Rev. Mod. Phys.*, **82** (2010) 789.
- [6] JACQUIN H., BERTHIER L. and ZAMPONI F., *Phys. Rev. Lett.*, **106** (2011) 135702.
- [7] DONEV A., TORQUATO S. and STILLINGER F. H., *Phys. Rev. E*, **71** (2005) 011105.
- [8] ZHANG Z., XU N., CHEN D. T. N., YUNKER P., ALSAYED A. M., APTOWICZ K. B., HABDAS P., LIU A. J., NAGEL S. R. and YODH A. G., *Nature*, **459** (2009) 230.
- [9] WANG L. and XU N., *ArXiv e-prints*, (2011).
- [10] CHENG X., *Phys. Rev. E*, **81** (2010) 031301.
- [11] OTSUKI M. and HAYAKAWA H., *Phys. Rev. E*, **86** (2012) 031505.
- [12] JACQUIN H. and BERTHIER L., *Soft Matter*, **6** (2010) 2970.
- [13] BERTHIER L., JACQUIN H. and ZAMPONI F., *Phys. Rev. E*, **84** (2011) 051103.
- [14] WYART M., NAGEL S. R. and WITTEN T. A., *EPL (Europhysics Letters)*, **72** (2005) 486.
- [15] STANLEY H. E., *Introduction to Phase Transitions and Critical Phenomena*. (Oxford University Press) 1971.
- [16] BRAZHKIN V. V., FOMIN Y. D., LYAPIN A. G., RYZHOV V. N. and TSIOK E. N., *J. Phys. Chem. B*, **115** (2011) 1411214115.
- [17] LECHENAULT F., DAUCHOT O., BIROLI G. and BOUCHAUD J. P., *EPL (Europhysics Letters)*, **83** (2008) 46003.
- [18] LECHENAULT F., DAUCHOT O., BIROLI G. and BOUCHAUD J. P., *EPL (Europhysics Letters)*, **83** (2008) 46002.

- [19] MAJMUDAR T. S. and BEHRINGER R. P., *Nature*, **435** (2005) 1079.
- [20] O'HERN C. S., LANGER S. A., LIU A. J. and NAGEL S. R., *Phys. Rev. Lett.*, **86** (2001) 111.
- [21] BERTHIER L., BIROLI G., BOUCHAUD J.-P., CIPELLETTI L. and SAARLOOS W. V., (Editors) *Dynamical Heterogeneities in Glasses, Colloids, and Granular Media* (Oxford University Press) 2011.
- [22] CHAUDHURI P., BERTHIER L. and SASTRY S., *Phys. Rev. Lett.*, **104** (2010) 165701.
- [23] IKEDA A., BERTHIER L. and BIROLI G., *arXiv eprint: 1209.2814*, (2012) .